GEOPHYSICS, VOL. 37, NO. 3 (JUNE 1972), P. 507-517, 7 FIGS, 1 TABLE

THE ANALYTIC SIGNAL OF TWO-DIMENSIONAL MAGNETIC BODIES WITH POLYGONAL CROSS-SECTION: ITS PROPERTIES AND USE FOR AUTOMATED ANOMALY INTERPRETATION†

MISAC N. NABIGHIAN*

This paper presents a procedure to resolve magnetic anomalies due to two-dimensional structures. The method assumes that all causative bodies have uniform magnetization and a cross-section which can be represented by a polygon of either finite or infinite depth extent.

The horizontal derivative of the field profile transforms the magnetization effect of these bodies of polygonal cross-section into the equivalent of thin magnetized sheets situated along the perimeter of the causative bodies. A simple transformation in the frequency domain yields an analytic function whose real part is the horizontal derivative of the field profile and whose imaginary part is the vertical derivative of the field profile. The latter can also be recognized as the Hilbert transform of the former. The procedure yields a fast and accurate way of computing the vertical derivative from a given profile.

For the case of a single sheet, the amplitude of the analytic function can be represented by a symmetrical function maximizing exactly over the top of the sheet. For the case of bodies with polygonal cross-section, such symmetrical amplitude functions can be recognized over each corner of each polygon. Reduction to the pole, if desired, can be accomplished by a simple integration of the analytic function, without any cumbersome transformations.

Narrow dikes and thin flat sheets, of thickness less than depth, where the equivalent magnetic sheets are close together, are treated in the same fashion using the field intensity as input data, rather than the horizontal derivative. The method can be adapted straightforwardly for computer treatment.

It is also shown that the analytic signal can be interpreted to represent a complex "field intensity," derivable by differentiation from a complex "potential." This function has simple poles at each polygon corner.

Finally, the Fourier spectrum due to finite or infinite thin sheets and steps is given in the Appendix.

INTRODUCTION

In the last few years, there have been numerous attempts to utilize computers for the automated anomaly resolution of two-dimensional structures (Hartman et al, 1971; O'Brien, 1971; Naudy, 1971). In all the published techniques, the emphasis is usually placed on initially presuming a given type body (vertical prisms, dikes, etc.) rather than allowing the body form to emerge. While some information could be gained by using such underlying assumptions, there are obvious limitations to these techniques.

A new method of magnetic anomaly resolution of two-dimensional structures follows. The only assumption made, besides uniform magnetization, is that the cross-sections of all causative bodies can be represented by polygons of finite or infinite depth extent.

The proposed technique makes extensive use of the concept of the analytic signal of a function. In our problem, the latter will be interpreted as a complex field intensity due to a complex potential.

† Manuscript received by the Editor November 15, 1971; revised manuscript received December 28, 1971.

* Newmont Exploration Limited, Danbury, Connecticut 06810.

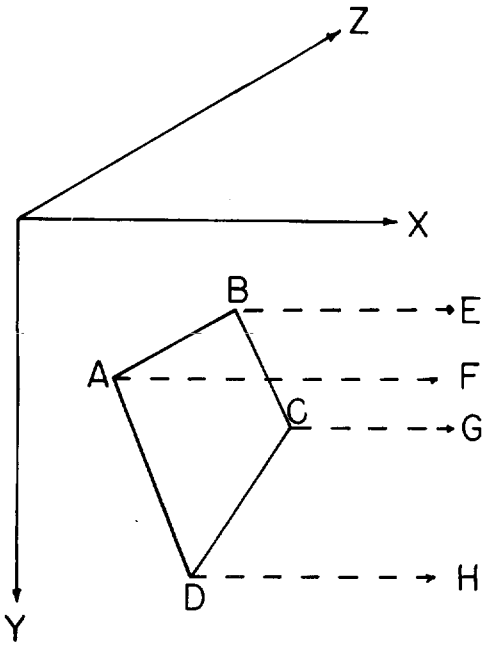

FIG. 1. Decomposition of a prismatic two-dimensional body ABCD into its step components.

All operations, although formally derivable through the use of the Hilbert transform, can be readily accomplished in the frequency domain by simple transformations. The advent of the fast Fourier transform techniques makes such operations economical.

FUNDAMENTAL RELATIONS AND SOLUTION OF THE PROBLEM

It is well known that any polygonal two-dimensional body (not necessarily depth limited) can be obtained by superimposing a finite number of magnetized steps. As seen in Figure 1, we have

$$\overline{ABCD} = \overline{ABEF} + \overline{DAFH} - \overline{CBEG} - \overline{DCGH},$$

where $\overline{ABCD}$ is the two-dimensional body with cross-section ABCD, representing a magnetized step of finite or infinite depth extent.

Since any depth-limited step can be obtained by subtracting two infinite depth-extent steps, we will concentrate our efforts primarily on the latter.

With the notations given in Figure 2, the anomaly ΔM due to a finite magnetized step can be written in the form:

$$\Delta M(x) = 2kFc \sin d \left[(\theta_1 - \theta_2) \cos \phi + \sin \phi \ln \frac{r_1}{r_2} \right], \quad (1)$$

where

k is the susceptibility contrast of the step;
F is the earth's magnetic field;
c and ϕ are given in Table 1;
i is the inclination of earth's field;
A is the angle between magnetic north and positive x axis; and
$\tan I = \tan i / \cos A$.

By differentiating (1) with respect to x and letting $t \to \infty$, we obtain the horizontal derivative,[1]

[1] Since in applications we let $y=0$, we write for simplicity $T(x)$ instead of $T(x, y)$.

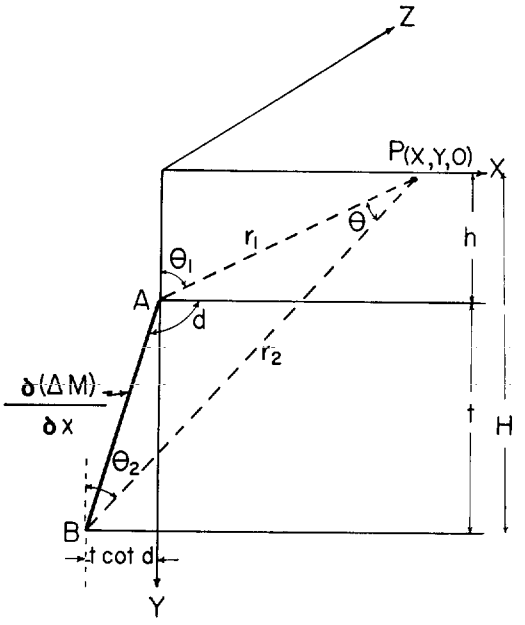

FIG. 2. Notation used to derive the magnetic anomaly due to a two-dimensional finite step. The heavy line labelled $\partial(\Delta M)/\partial x$ represents the finite thin sheet which gives an anomaly equal to the horizontal derivative of the step anomaly.

Table 1. c and ϕ for total, vertical, and horizontal fields

	For total field anomaly	For vertical field anomaly	For horizontal field anomaly
c	$1-\cos^2 i \sin^2 A$	$(1-\cos^2 i \sin^2 A)^{\frac{1}{2}}$	$\cos A\,(1-\cos^2 i \sin^2 A)^{\frac{1}{2}}$
ϕ	$2I-d-90$	$I-d$	$I-d-90$

$$T(x) = \frac{\partial(\Delta M)}{\partial x} = 2kFc \sin d \frac{(h-y)\cos\phi + x\sin\phi}{(h-y)^2 + x^2}, \tag{2}$$

representing the anomaly of a thin infinite sheet (AB in Figure 2) at depth h, dipping at an angle d. Similarly, differentiating equation (1) with respect to y yields for $t \to \infty$ the vertical derivative

$$T_1(x) = \frac{\partial(\Delta M)}{\partial y} = 2kFc \sin d \frac{x\cos\phi - (h-y)\sin\phi}{(h-y)^2 + x^2} \tag{3}$$

In what follows, extensive use will be made of the Hilbert transform pair defined by the relations:

$$g(\xi) = \frac{1}{\pi} \barint_{-\infty}^{\infty} \frac{F(x)}{x-\xi}\,dx \quad \text{and} \qquad F(x) = \frac{1}{\pi} \barint_{-\infty}^{\infty} \frac{g(\xi)}{x-\xi}\,d\xi, \tag{4}$$

where the bar on the integral sign $\int$ implies principal value.

Using (4), we have (Erdelyi and Magnus et al, 1954, p. 245)

$$\frac{1}{x^2+h^2} \leftrightarrow -\frac{\xi}{h(\xi^2+h^2)} \quad \text{and} \qquad \frac{x}{x^2+h^2} \leftrightarrow \frac{h}{\xi^2+h^2}, \tag{5}$$

where $\leftrightarrow$ signifies Hilbert transformation.

With (5) it is easy to see that $T_1(x)$ given by (3) is the negative of the Hilbert transform of $T(x)$, given by (2), i.e.,

$$T(x) \leftrightarrow -T_1(\xi). \tag{6}$$

Thus relation (6) allows the determination of the vertical derivative of ΔM from its horizontal derivative, in a very straightforward fashion.

Such a derivation is more easily accomplished in the frequency domain. Indeed, if $F(w)$ is the Fourier transform of $T(x)$, the Fourier transform $F_1(w)$ of $T_1(x)$ is given by (Whalen, 1971, p. 62):

$$F_1(w) = i\,\text{sgn}\,(w) F(w), \tag{7}$$

where

$$\text{sgn}\,(w) = \begin{cases} 1 & \text{for } w > 0 \\ 0 & \text{for } w = 0 \\ -1 & \text{for } w < 0 \end{cases}$$

and

$$i = \sqrt{-1}.$$

Relation (7) gives a simple way of determining $T_1(x)$ as the inverse transform of $F_1(w)$. However, for what follows, it is convenient to introduce and use the concept of analytic signal from communication theory (Whalen, 1971, p. 69).

To this end, from the Fourier transform $F(w)$ of $T(x)$, we may create a new spectrum defined by

$$\tilde{F}(w) = \begin{cases} 2F(w) & \text{for } w > 0 \\ F(w) & \text{for } w = 0 \\ 0 & \text{for } w < 0, \end{cases} \tag{8}$$

i.e., we double the positive frequencies, cancel the negative ones, and leave the dc level unchanged.

From (7) and (8), it is easy to see that the inverse Fourier transform of $\tilde{F}(w)$ is the function $A(x) = T(x) - iT_1(x)$.

Using (A6) from the Appendix, together with (2) and (3), we can write the Fourier transform pair.

$$A(x) = \frac{\alpha e^{i\phi}}{(h-y)+ix} \leftrightarrow \begin{cases} 2\pi\alpha e^{i\phi} e^{-wh} & \text{for } w > 0 \\ \pi\alpha e^{i\phi} & \text{for } w = 0 \\ 0 & \text{for } w < 0, \end{cases} \tag{9}$$

where $\alpha = 2kFc \sin d$.

The function $A(x)$ has a number of interesting properties, which can be recognized:

1) It is an analytic function of the complex variable $z = x + iy$,

$$A(z) = \frac{\alpha e^{i\phi}}{h + iz}, \qquad (10)^2$$

whose real and imaginary parts satisfy the Cauchy-Riemann conditions

$$\frac{\partial T}{\partial x} = -\frac{\partial T_1}{\partial y}$$
$$\frac{\partial T}{\partial y} = \frac{\partial T_1}{\partial x}. \qquad (11)$$

2) Its amplitude is a symmetric function with respect to $x = 0$, which does not depend on ϕ:

$$|A(z)| = (T^2 + T_1^2)^{1/2}$$
$$= \frac{\alpha}{[(h - y)^2 + x^2]^{1/2}}$$
$$\rightarrow \frac{\alpha}{[h^2 + x^2]^{1/2}}. \qquad (12)$$

The arrow in the above expression signifies the limiting case for $y = 0$, which is the only one of interest.

3) It is the derivative of a complex "potential" which can be written in the general form

$$W(x, y) = U(x, y) + iV(x, y), \qquad (13)$$

which is analytic everywhere except at the sources.

The functions $U(x, y)$ and $V(x, y)$ satisfy the Cauchy-Riemann relations

$$\frac{\partial U}{\partial x} = \frac{\partial V}{\partial y}$$
$$\frac{\partial U}{\partial y} = -\frac{\partial V}{\partial x}. \qquad (14)$$

From (13) and (14), it is easy to see that if we let

$$T(x) = -\frac{\partial U}{\partial x} = -\frac{\partial V}{\partial y}$$

and

$$T_1(x) = -\frac{\partial U}{\partial y} = \frac{\partial V}{\partial x}, \qquad (15)$$

we can write

$$A(z) = -\frac{\partial W(z)}{\partial z} = -\left[\frac{\partial U}{\partial x} + i\frac{\partial V}{\partial x}\right]$$
$$= T(x) - iT_1(x). \qquad (16)$$

Thus the function $T(x) - iT_1(x)$ can be considered to represent the complex field intensity due to the complex potential $W(z)$.

Some straightforward algebra leads us to the following expressions for the functions $U(x, y)$, $V(x, y)$, and $W(x, y)$:

$$U(x, y) = \alpha\left\{\cos\phi \tan^{-1}\frac{x}{y-h} - \sin\phi \ln\left[x^2 + (h-y)^2\right]^{1/2}\right\},$$

$$V(x, y) = \alpha\left\{\sin\phi \tan^{-1}\frac{x}{y-h} + \cos\phi \ln\left[x^2 + (h-y)^2\right]^{1/2}\right\}, \qquad (17)$$

and

$$W(x, y) = \alpha e^{i\phi}\left\{\tan^{-1}\frac{x}{y-h} + i \ln\left[x^2 + (h-y)^2\right]^{1/2}\right\}.$$

4) From (10) it follows that, in general, the complex field intensity $A(z)$ has simple poles at each corner of each polygon. (Or, conversely, the function $1/A(z)$ has zeros at those points.) This can lead by itself to a method of solution to our problem, since the location of the poles and their residues yield all information of interest.

[2] The complex variable $z = x + iy$ should not be confused with the z coordinate (Figure 2) which does not enter the picture.

5) The bell-shaped function

$$a(x) = |A(z)|^2 = T^2(x) + T_1^2(x) = \frac{\alpha^2}{h^2 + x^2}$$

has the property that its half-maximum half-width is equal to h (see Figure 3). Also the 4/5 and 1/5 amplitude points have half-maximum half-widths of $h/2$ and $2h$ and they intersect the $a(x)$ curve along a straight line passing through the maxima. The latter is situated right above the corresponding corner of the polygonal surface.[3]

6) If we introduce a frequency shifting in (8), i.e., we replace $\tilde{F}(w)$ by $\tilde{F}(w+s)$, we obtain, by using (9),

$$\tilde{F}(w + s) = e^{-sh}\tilde{F}(w). \qquad (18)$$

The inverse transformation of (18) yields

$$|A(z)|_s^2 = e^{-2sh}|A(z)|^2. \qquad (19)$$

where $|A(z)|_s^2$ is the amplitude square of the complex field intensity obtained after shifting the spectrum by s units. In other words, a frequency shifting as given by (18) is translated into an exponential attenuation ($s>0$) or amplification ($s<0$) of the amplitude of the complex field intensity. This could be used to determine h.

7) By using (5), we can Hilbert transform the $a(x)$ function to obtain

$$\frac{\alpha^2}{h^2 + x^2} \leftrightarrow -\frac{\alpha^2}{h}\frac{\xi}{h^2 + \xi^2} = |A_1(z)|^2 = a_1(\xi). \qquad (20)$$

From the above, we deduce

$$a_1(x) = -\frac{x}{h}a(x)$$

[3] It is worth mentioning that "bell-shaped" symmetrical functions could be obtained in a variety of ways. A simple approach is given for instance by the relations

$$T(x)\frac{\partial T_1(x)}{\partial x} - T_1(x)\frac{\partial T(x)}{\partial x} = \frac{\alpha^2 h}{(h^2 + x^2)^2},$$

or

$$\left(\frac{\partial^n T}{\partial x^n}\right)^2 + \left(\frac{\partial^n T_2}{\partial x^n}\right)^2 = \frac{(1^2 \cdot 2^2 \cdots n^2)\alpha^2}{(h^2 + x^2)^{n+1}}$$

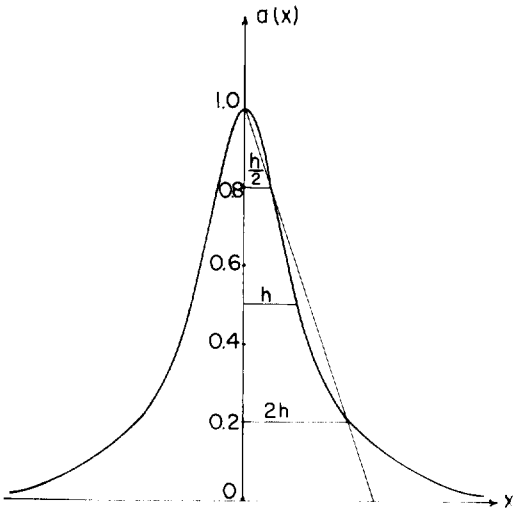

FIG. 3. The amplitude curve $a(x) = T^2(x) + T_1^2(x)$ of the analytic signal. The units are arbitrary.

or

$$\frac{d}{dx}\left[-\frac{a_1(x)}{a(x)}\right] = \frac{1}{h}, \qquad (21)$$

which also yields h. A number of other procedures to determine the depth h could be found easily.

8) At $x=0$, the $a(x)$ function attains a maximum equal to α^2/h^2. Once h is determined from (19) or (21), we thus obtain α and hence the susceptibility k. At the same point, the $T(x)$ curve has the value

$$T(0) = \frac{\alpha \cos \phi}{h}. \qquad (22)$$

We have α^2/h^2 (and hence α/h) from the amplitude curve and obtain from (22) the angle ϕ and hence the dip d, etc.

9) Using the known orthogonality relation between a function and its Hilbert transform, we have

$$\int_{-\infty}^{\infty} T(x)T_1(x)dx = 0$$

and (23)

$$\int_{-\infty}^{\infty} a(x)a_1(x)dx = 0.$$

10) The following relations can easily be proven:

$$\int_{x_1}^{x_2} a(x)a_1(x)dx = \frac{\alpha^2}{2h}\left[\frac{1}{h^2+x_2^2} - \frac{1}{h^2+x_1^2}\right] = \frac{\alpha^2}{2h}[a(x_2) - a(x_1)], \quad (24)$$

which yields $\alpha^2/2h$.
Also

$$a^2(x) + a_1^2(x) = \frac{\alpha^2}{h^2}a(x), \quad (25)$$

which yields α^2/h^2.
Additional properties may be derived. However, the above relations are more than enough to solve our problem.

In general, we proceed as follows:

1) The field curve (whether horizontal, vertical, or total component) is differentiated with respect to x to yield $T(x)$. Any constant "normal field" or "level" in the initial data is thus removed.
2) The latter is Fourier transformed to yield $F(w)$.
3) We use (8) to create the new spectrum $\tilde{F}(w)$.
4) Inverse transformation of the above yields $T(x) - iT_1(x)$.
5) The amplitude square $a(x) = T^2(x) + T_1^2(x)$ is plotted (or stored in the memory of the computer). This curve represents a symmetric bell-shaped function, situated exactly over the top of the sheet and with a half-maximum half-width equal to h.
6) Using any of the relations (18) through (25), we obtain h, α or k, ϕ or d, etc.
7) If there are thin elongated bodies in the geologic section (thin dikes, thin flat sheets, etc.) of thickness less than depth, the equivalent magnetic sheets will be closer together. In such cases, the procedure is similar to the one outlined above with the exception that the field intensity curve is used as input data, rather than the horizontal derivative. Usually both computations are done sequentially. In regions where thin formations are present, there will be a high correlation between their respective amplitude curves.

For the general case of a geologic cross-section which can be represented by a number of bodies of polygonal cross-section, the procedure is identical to the one outlined above. Each corner of each polygon will contribute primarily a symmetric component to the total amplitude curve $a(x)$. By recognizing and interpreting such symmetric components, a reliable estimation of the physical and geometrical parameters of each body could be achieved.

As an example, the amplitude curve obtained by the above procedure over a two-dimensional trapezoidal body is given in Figure 4. We can easily recognize the symmetric components of this curve. As expected, all components peak over the corresponding corner and have a half-maximum half-width equal to h. (The deeper the corner, the wider the corresponding curve.)

REDUCTION TO THE POLE

The expressions developed so far could also be used for reduction to the pole.

To this end, we note from (2) and (3) that

$$T(x)\big|_{\phi_1 \pm \phi_2} = \cos\phi_2 T(x)\big|_{\phi_1} \pm \sin\phi_2 T_1(x)\big|_{\phi_1}, \quad (26)$$

$$T_1(x)\big|_{\phi_1 \mp \phi_2} = \cos\phi_2 T_1(x)\big|_{\phi_1} \pm \sin\phi_2 T(x)\big|_{\phi_1}, \quad (27)$$

and

$$[T(x) - iT_1(x)]\big|_{\phi_1 \mp \phi_2} = [T(x) - iT_1(x)]\big|_{\phi_1 e^{\pm i\phi_2}}, \quad (28)$$

where $T(x)\big|_\phi$ and $T_1(x)\big|_\phi$ represent the derivative functions computed for the angle ϕ.

Taking into account that, at the pole, we have $I = 90$ degrees, we note from Table 1 that in order to accomplish a reduction to the pole, we have to increase the angle ϕ_1 by

$$\phi_2 = 180 - 2I \text{ for total field anomalies, and}$$
$$\phi_2 = 90 - I \text{ for vertical and horizontal field anomalies.} \quad (29)$$

Since I, and hence ϕ_2, are known, we obtain from (26)

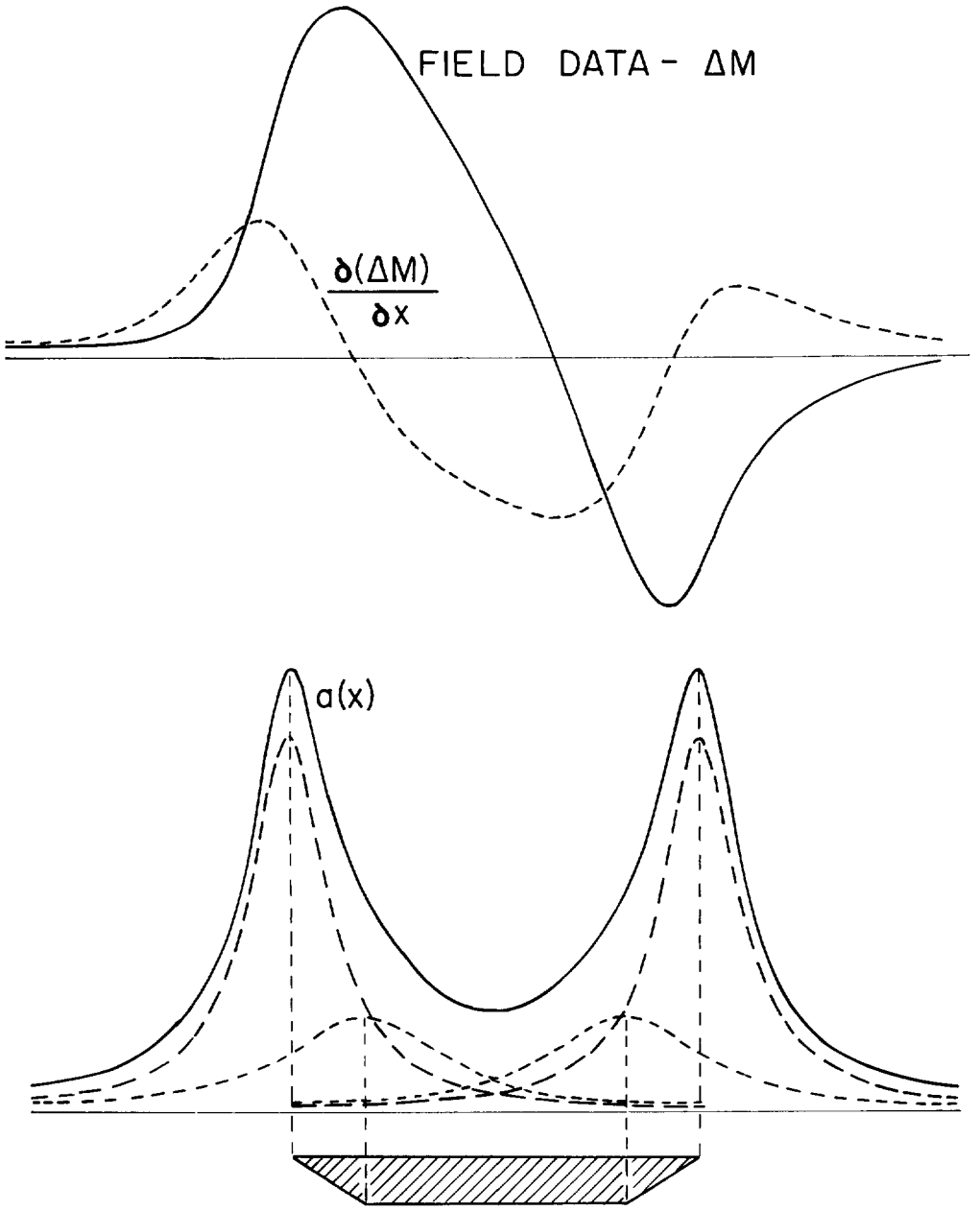

FIG. 4. Theoretical model. Total field anomaly, its horizontal derivative and the analytic signal amplitude of a trapezoidal body. The units are arbitrary. The symmetric components of the amplitude curve are shown in dashed line.

$$T(x)\,|_{\text{pole}} = \cos\phi_2 T(x) + \sin\phi_2 T_1(x). \quad (30)$$

The original field profile reduced to the pole is then obtained by integrating (30) over x, i.e.,

$$\Delta M(x)\,|_{\text{pole}} = \int [\cos\phi_2 T(x) + \sin\phi_2 T_1(x)]\,dx, \quad (31)$$

or, equivalently,

$$\Delta M(x)\,|_{\text{pole}} = \text{Real part of} \int [T(x) - iT_1(x)]e^{i\phi_2}dx. \quad (32)$$

The anomaly, reduced to the pole, computed from (31) for the previously used trapezoidal body is shown in Figure 5.

To the writer's knowledge, relations (31) and (32) appear for the first time in publications of applied geophysics. They are remarkable in their simplicity.

DISCUSSION

It is the opinion of the writer that locating the position of the corners of each polygon is the most important step toward the solution of our problem.

As can be seen readily, the success of the proposed technique depends largely on the accuracy with which we can recognize symmetric components in the amplitude $a(x)$ curve. Such a separation can be done in a variety of ways, from visual inspection to crosscorrelation techniques.

An interesting approach to this problem consists of computing at each point of the $a(x)$ curve its symmetric (even) and antisymmetric (odd) parts. It can easily be shown that the integral of the absolute value of the odd part

$$\int_{-\infty}^{\infty} |\text{ odd } a(x)\,|\,dx \quad (33)$$

has a localized minimum value whenever the separation into even and odd components is accomplished above a polygon corner.

Once the location of the poles on the profile (and of their number) is established, a first approximation of the α and h values of each corner is obtained from the $a(x)$, $T(x)$, and $T_1(x)$ curves and using (18) through (25).

The values so determined are used as a starting solution in an iterative nonlinear optimization technique to yield the best decomposition possible of the $a(x)$ curve into symmetric components (in the least-square sense). The final values give the best solution to our problem.

When bodies of finite polygonal shape are present in the geologic cross-section, the values of α so determined represent, in fact, the combined sum of two α values, one for each of the polygon sides that make that corner. For instance in Figure 1, the $\bar{\alpha}_B$ value determined for the corner B, will result from the α_{AB} and α_{BC} values due to the sides AB and BC.

Since any finite magnetized sheet can be obtained by subtracting two infinite sheets, we can consider the resultant α values for each corner to represent the combined effect of two infinite sheets of opposite polarity.

Noting that in expression (2) the thickness of an infinite sheet is given by $\sin d$, it can be shown easily that the combined effect of two infinite sheets of opposite polarity and dips d_1 and d_2 is the same as that given by a single infinite sheet of the same susceptibility, but dipping at an angle (d_1+d_2) and of thickness $\sin(d_1-d_2)$, i.e.,

$$2kFc \sin d_1 \frac{h\cos\phi_1 + x\sin\phi_1}{h^2 + x^2} - 2kFc \sin d_2 \frac{h\cos\phi_2 + x\sin\phi_2}{h^2 + x^2} \quad (34)$$

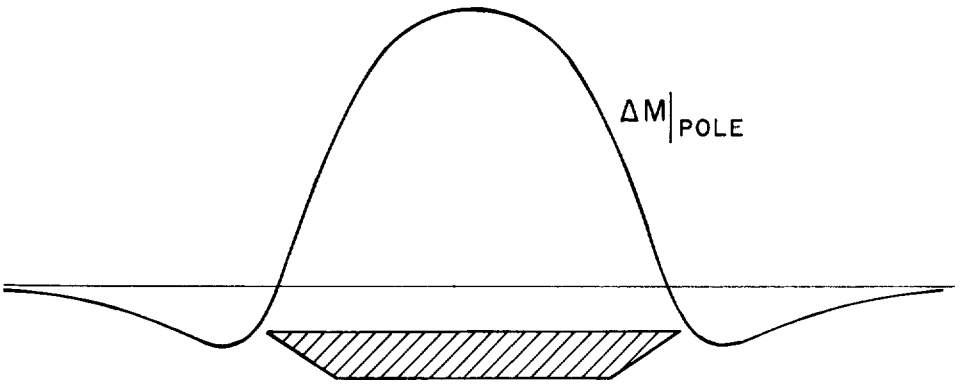

FIG. 5. Theoretical model. Trapezoidal body. Anomaly reduced to the pole (units are arbitrary).

$$= 2kFc \sin (d_1 - d_2) \frac{h \cos \bar{\phi} + x \sin \bar{\phi}}{h^2 + x^2},$$

where $\bar{\phi}$ is computed for an apparent dip $d = d_1 + d_2$, whereas ϕ_1 and ϕ_2 are computed for true dips d_1 and d_2.

Using (34), we obtain for the corner B in Figure 1

$$\begin{aligned} \bar{\alpha}_B &= 2kFc \sin (d_{BA} - d_{BC}) \\ d_B &= d_{BA} + d_{BC}. \end{aligned} \tag{35}$$

Similar relations can be derived for the other corners, leading in general to a system of equations from which k can be determined. (The dips are determined directly from the way we connected the corners.)

In this fashion, location, depth, and strength of each pole is easily determined.

Because the vertical derivative and the anomaly reduced to the pole are obtained without any significant effort, we have at our disposal a whole series of curves to facilitate the proper connection of the polygon corners between them.

A field example taken from the airborne magnetic survey of the Ely, Nevada area is shown in Figures 6 and 7. The profile chosen for interpretation coincides with a flight line to minimize interpolation errors. The target, in this case, is an outcropping monzonite porphyry intrusive in a limestone and shale environment. As can be seen from the magnetic map, the conditions are not ideal; the structures are only approximately two-dimensional (there is a large widening toward the northeast of the intrusive).

The technique was applied to the total field data without any heavy smoothing. The resultant curves are shown in Figure 7.

As can be seen from the amplitude $a(x)$ curve, in the central part of the anomaly, apparently four corners are present. However, when optimization is attempted, the leftmost corner is rejected and only three corners are kept, yielding the body drawn at the bottom of the figure. The resultant amplitude curve (dotted in the figure) is in close agreement with the observed one. The anomaly reduced to the pole indicates that the way we connected the poles is valid.

Note that a heavier smoothing on the field data would eliminate the leftmost determined pole.

The $T_1(x)$ and $a(x)$ curves and the anomaly reduced to the pole were determined directly from the relations given in text. No smoothing whatsoever was involved in the process.

The concepts of complex potential and complex field intensity provide additional insight into the problem. Although not new (see Kogbetliantz, 1944; Strakhov, 1956), these concepts were, for the first time, applied in the frequency domain and to quantities derivable from a single field component measurement, horizontal, vertical, or total. Thus the proposed technique is applicable to most situations encountered in magnetic exploration.

It is worth mentioning that the extension of the present theory to gravimetric anomalies as well as the three-dimensional case does not present any particular difficulties, since practically all such bodies exhibit spectral characteristics analogous to the ones for the thin sheet. The three-dimensional treatment will be the subject of a future paper.

APPENDIX

FOURIER SPECTRUM OF THIN SHEETS AND FINITE OR INFINITE STEPS

1) *Thin infinite sheet*

From (2) the anomaly due to a thin sheet situated at a depth h and dipping at an angle d is given by (for $y = 0$)

$$T(x) = \alpha \frac{h \cos \phi + x \sin \phi}{h^2 + x^2}, \tag{A1}$$

where $\alpha = 2kFc \sin d$.

Letting

$$F(w) = \int_{-\infty}^{\infty} T(x) e^{iwx} dx,$$

we obtain, after some simple algebra, the amplitude spectrum of a thin sheet in the form

$$F(w) = \begin{cases} \pi\alpha e^{i\phi} e^{-wh} & \text{for } w > 0 \\ \pi\alpha \cos \phi & \text{for } w = 0 \\ \pi\alpha e^{-i\phi} e^{wh} & \text{for } w < 0 \end{cases} \tag{A2}$$

or in a compact form for $w \neq 0$[4]

$$F(w) = \pi\alpha e^{i\phi \operatorname{sgn}(w)} e^{-|w|h}. \tag{A3}$$

[4] In (A3) and some following relations the value of $F(w)$ for $w = 0$ is obtained from the Dirichlet condition

$$F(0) = \tfrac{1}{2}[F(0_+) + F(0_-)].$$

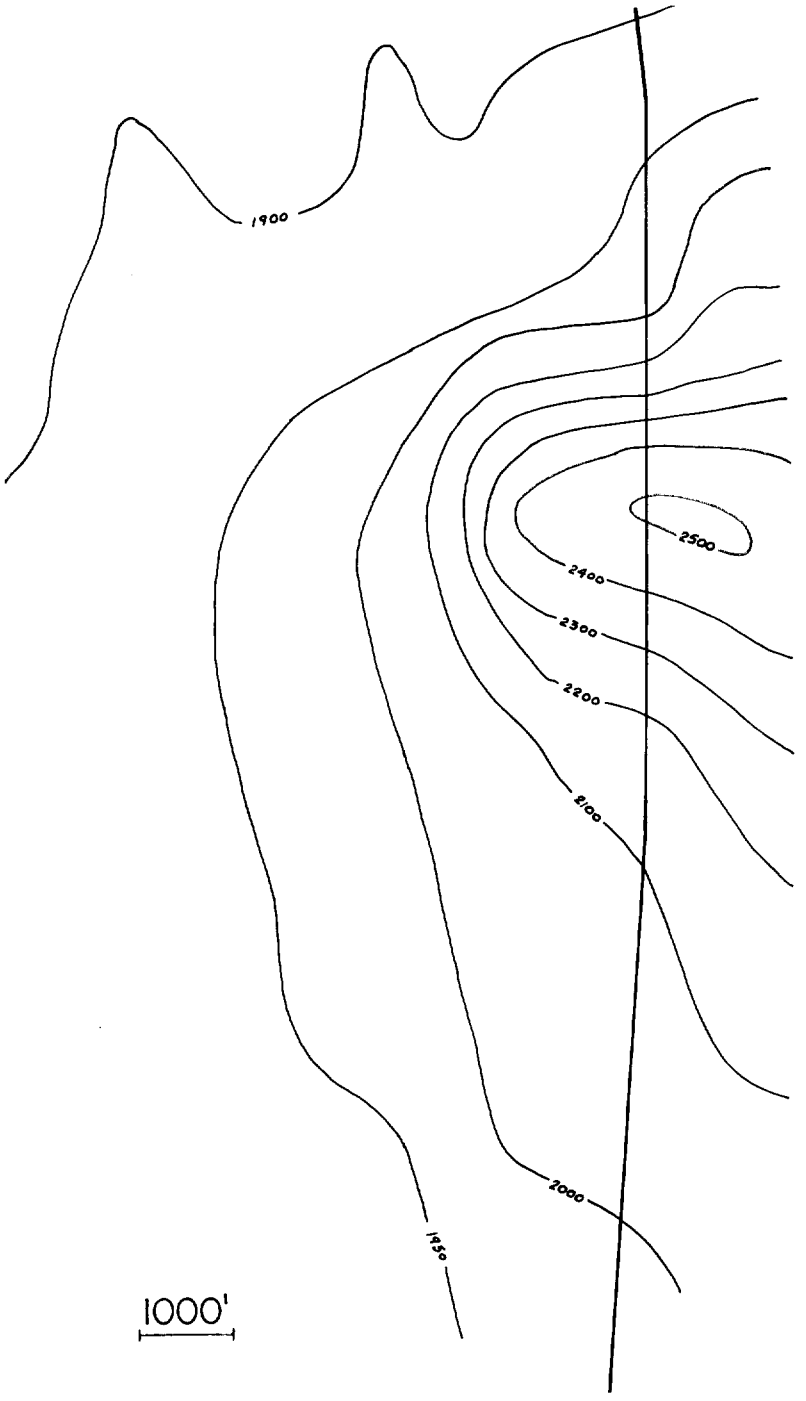

FIG. 6. Aeromagnetic map, Ely, Nevada area, showing the profile analyzed by the present technique.

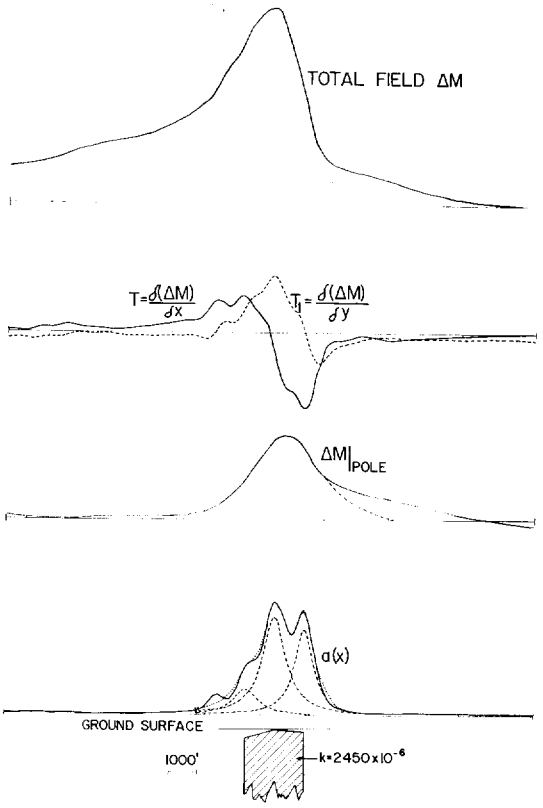

FIG. 7. Input and processed data for the profile shown in Figure 6. Symmetrical components of the $a(x)$ curve are shown in dashed line. The effect of the northeast extension of the intrusive is shown in dashed line on the anomaly reduced to the pole curve. The units and zero levels are arbitrary.

Using (7), the amplitude spectrum of the Hilbert transform of $T(x)$ is given by

$$F_1(w) = \begin{cases} i\pi\alpha e^{i\phi}e^{-wh} & \text{for } w > 0 \\ -\pi\alpha \sin\phi & \text{for } w = 0 \\ -i\pi\alpha e^{-i\phi}e^{wh} & \text{for } w < 0 \end{cases} \quad \text{(A4)}$$

or, in a compact form,

$$F_1(w) = i\pi\alpha \operatorname{sgn}(w) e^{i\phi \operatorname{sgn}(w)} e^{-|w|h}. \quad \text{(A5)}$$

From (A2) and (A4), we can write the transform pair

$$T(x) - iT_1(x) \leftrightarrow \tilde{F}(w) = \begin{cases} 2\pi\alpha e^{i\phi}e^{-wh} & \text{for } w > 0 \\ \pi\alpha e^{i\phi} & \text{for } w = 0 \\ 0 & \text{for } w < 0. \end{cases} \quad \text{(A6)}$$

2) *Thin finite sheet*

A finite sheet can be obtained by subtracting two infinite sheets. With the notation given in Figure 2 and using the known shifting property of the Fourier transform, we obtain

$$T_f(x) \leftrightarrow \pi\alpha\left[e^{-|w|h} - e^{iwt\cot d}e^{-|w|H}\right] \cdot e^{i\phi \operatorname{sgn}(w)}, \quad \text{(A7)}$$

where the subscript f implies finite (sheet).

3) *Infinite step*

The expression for the infinite step can be obtained by formally integrating over x the expression for an infinite thin sheet. Using a known relation between the Fourier transform of a function and that of its integral, we obtain in a straightforward fashion

$$\Delta M(w) = -\frac{\pi\alpha}{iw} e^{-|w|h}e^{i\phi \operatorname{sgn}(w)}. \quad \text{(A8)}$$

4) *Finite step*

As in the case of the finite sheet, a suitable subtraction of two infinite steps yields

$$\Delta M_f(w) = -\frac{\pi\alpha}{iw}\left[e^{-|w|h} - e^{iwt\cot d}e^{-|w|H}\right] \cdot e^{i\phi \operatorname{sgn}(w)}. \quad \text{(A9)}$$

ACKNOWLEDGMENT

The author is deeply grateful to Dr. A. A. Brant, director of Newmont Exploration Limited, for actively encouraging this research and for permission to publish the results.

REFERENCES

Erdelyi, A., and Magnus, W., et al, 1954, Table of integral transforms, Vol. II: New York, McGraw-Hill Book Co., Inc.

Hartman, R. R., Teskey, D., and Friedberg, J. L., 1971, A system for rapid digital aeromagnetic interpretation: Geophysics, v. 36, p. 891–918.

Kogbetliantz, E. G., 1944, Quantitative interpretation of magnetic and gravitational anomalies: Geophysics, v. 9, p. 463–493.

Naudy, H., 1971, Automatic determination of depth on aeromagnetic profiles: Geophysics, v. 36, p. 717–722.

O'Brien, D. P., 1971, An automated method of magnetic anomaly resolution and depth-to-source computation: Symposium, Berkeley, California.

Strakhov, V. N., 1956, Determination of some basic parameters of magnetized bodies from magnetic data (in Russian): Izvestia Academii Nauk, USSR, Geophysics Series, no. 2, p. 144–156.

Whalen, A. D., 1971, Detection of signals in noise: New York, Academic Press.